The Egyptian Journal of Radiology and Nuclear Medicine (2016) 47, 325–333

Egyptian Society of Radiology and Nuclear Medicine

The Egyptian Journal of Radiology and Nuclear Medicine

www.elsevier.com/locate/ejrnm
www.sciencedirect.com

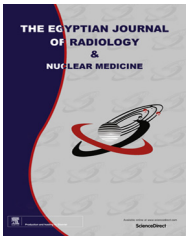

ORIGINAL ARTICLE

Usefulness of diffusion-weighted magnetic resonance imaging for the characterization of benign and malignant renal lesions

Sally Emad-Eldin [a,*], Shady Rakha [a], Sameh A.Z. Hanna [a], Hesham Badawy [b]

[a] Diagnostic and Intervention Radiology Department, Cairo University Hospitals, Kasr Al-Ainy, Cairo, Egypt
[b] Urology Department, Cairo University Hospitals, Kasr Al-Ainy, Cairo, Egypt

Received 29 May 2015; accepted 6 October 2015
Available online 20 October 2015

KEYWORDS

DWI;
Renal;
Benign;
Malignant

Abstract *Purpose:* Our aim was to evaluate the diagnostic potential of diffusion-weighted magnetic resonance imaging (DW-MRI) and quantitative assessment of apparent diffusion coefficient (ADC) value for the characterization of renal lesions and differentiation into benign and malignant.
Patients and methods: A total of 87 consecutive patients with 107 renal lesions were enrolled in this prospective study. MRI examinations including DWI with *b* factors of 0, 600 and 800 s/mm^2 were performed at 1.5 T MRI unit. The mean ADC values of normal renal parenchyma, solid and cystic lesions were calculated.
Results: There was statistical significance difference between ADC value of normal renal parenchyma with that of benign (n = 60, 56%) and malignant (n = 47, 44%) renal lesions (P value < 0.0001). ADC values differed significantly between solid (n = 74, 69.2%) and cystic lesions (n = 33, 30.8%) (P value < 0.0001). There was significant difference between ADC values of all benign (n = 60, 56%) and malignant renal lesions (n = 47, 44%) (P value < 0.0001) but not between benign solid (n = 27, 36.5%) and malignant solid renal lesions (n = 47, 63.5%) (P value = 0.784).
Conclusion: There is overlap between the ADC values of benign and malignant lesions. The use of ADC value alone may lead to inaccurate assessment of renal lesions. Thus, DW-MRI should be interpreted in conjunction with conventional MRI sequences to allow for better characterization of renal lesions.

1. Introduction

Accurate assessment of renal masses is important for establishing whether tumors require surgical intervention or not. Computed tomography (CT) and magnetic resonance imaging (MRI) are the primary investigative tools for diagnosing,

* Corresponding author at: Diagnostic and Intervention Radiology Department, Cairo University Hospitals, El-Manial, 11956 Cairo, Egypt. Tel.: +20 1061616935; fax: +20 2 236445464.
E-mail address: sallyemad@hotmail.com (S. Emad-Eldin).
Peer review under responsibility of Egyptian Society of Radiology and Nuclear Medicine.

http://dx.doi.org/10.1016/j.ejrnm.2015.10.005

characterizing, and staging cystic or solid renal masses discovered incidentally by ultrasonography (1). However, MRI further characterized a large proportion of renal masses that were considered indeterminate at CT (2).

Diffusion weighted magnetic resonance imaging (DW-MRI) is a reasonable alternative to conventional cross sectional imaging to detect and characterize focal renal lesions, especially in patients with impaired renal function (3). The diffusion characteristics can be measured objectively and are represented in the form of apparent diffusion coefficient (ADC) values. So tissue diffusivity and, hence, diffusion-weighted imaging (DWI) can provide crucial diagnostic information regarding the architecture of various tissues and organs (4).

The aim of this study was to evaluate the diagnostic potential of DW-MRI and quantitative assessment of ADC value for the characterization of renal lesions and differentiation into benign and malignant.

2. Patients and methods

2.1. Patients

The study was approved by the hospital ethical committee, and an informed consent was obtained from all patients. During 2 years duration, we prospectively evaluated 87 consecutive patients (41 females, 46 males). They ranged in age from 15 to 71 years (mean 49.86 ± 15.82 year). All patients underwent renal MR imaging which included DWI for further evaluation and characterization of renal lesions previously detected by US and/or CT.

2.2. Methods

The MRI examinations were performed with a 1.5-T MRI system using two different MRI machines (Intera and Achieva; Philips Medical Systems, the Netherlands) equipped with a phased array body coil. For morphologic evaluation of the kidneys, respiratory triggered axial and coronal T2-weighted FSE sequences, axial T2-weighted spectral presaturation with inversion recovery (SPIR) with fat suppression was initially performed, followed by axial T1-weighted SE, and T1-weighted dual-echo in-phase and out-of-phase sequences. A bolus of 0.1 mmol/kg of gadopentetate dimeglumine-DTPA (Magnevist; Schering, Berlin, Germany) was injected intravenously followed by 20-mL saline flush. Three-dimensional fat-saturation T1-weighted dynamic contrast-enhanced sequences were performed during suspended respiration at baseline (pre-contrast), during the arterial phase, and 30 and 120–240 s after the arterial phase. Gadolinium was not administrated in 6 cases due to impaired renal function. MRI imaging protocol is demonstrated in Table 1.

Axial DWI was obtained by using a single-shot spin echo-planar sequence prior to the administration of contrast material. DWI was acquired with b value of 0, 600 and 800 s/mm^2.

2.3. Image analysis

All MRI images were transferred to an independent workstation (Philips MR extended workspace, software version 2009). Image interpretation and diagnosis were carried out by two radiologists (11 and 15 years experience in abdominal MRI imaging). After interpretation by Radiologist 1, Radiologist 2 confirmed the diagnosis, and in case of controversy, they discussed to reach a consensus.

First the conventional MRI images, including un-enhanced and contrast enhanced images were reviewed. The morphological features of each lesion were recorded including number, site, size, shape, together with signal characteristics, and enhancing pattern.

Based on conventional MRI findings, renal lesions were divided into solid and cystic groups. Cystic renal lesions were classified according to the Bosniak classification system (I, II, II F, III and IV), and Bosniak category IV lesions were evaluated in the solid group (5,6).

The DWI images, including the images obtained with b values of 0, 600, and 800 s/mm^2, were reviewed together. ADC values were measured for b value of 800 s/mm^2 by using circumferential region of interest (ROI). Necrotic portions or lesion margins were excluded from the ROIs. At least three measurements were performed and the lowest value was recorded for each b value. Circular ROIs were placed in the normal renal parenchyma (at the central portion of the kidney) for the measurement of ADC values.

2.4. Standard of references

The findings obtained using conventional MRI and DWI were compared with the results of the histopathological findings, clinical and imaging follow-up.

2.5. Statistical analysis

All statistical calculations were performed using SPSS software (version 21; SPSS Inc., Chicago, IL, USA). Comparison

Table 1 Magnetic resonance imaging protocol.

MR sequence	TR/TE (m sec)	Flip angle (°)	Slice thickness (mm)	Slice gap (mm)	NEX	Fat suppression	FOV (mm)
1-Axial T1 SE	425/15	90	7–8	1–2	1	–	350 × 275
2-Coronal T2 HASTE	1100/120	90	7–8	1–2	2	yes	360 × 140
3-Axial T1-out-of-phase	75-100/2.3	10	7–8	–	1	–	350 × 275
In-phase	75-100/4.6	10	7–8	–	1	–	350 × 275
4-Axial T2 TSE	4360/95	90	7	1–2	1	–	350 × 275
5-Axial T2 SPAIR	2000/80	90	7	1–2	1	yes	350 × 275
6-Axial T1 3D GRE	3.4/1.7	10	6	–	1	yes	350 × 275
7-DWI-B value 0, 600, 800	1500/80	90	6	–	4	yes	190 × 115

TSE, turbo spin echo; GRE, gradient recalled echo; DW, Diffusion-weighted; TE, echo time; TR, repetition time.

between mean values of ADC in studied groups was performed using Student's-*t*-test. Standard diagnostic indices including sensitivity, specificity, positive predictive value (PPV), negative predictive value (NPV) and diagnostic efficacy were calculated. Receiver operating characteristic (ROC) curves were drawn to find out the area under the curve (AUC) for differentiation of two groups and cutoff ADC values were calculated in-order to achieve the highest average sensitivity and specificity. *P* value less or equal to 0.05 was considered significant and less than 0.01 was considered highly significant.

3. Results

3.1. Lesions characteristics

107 lesions in 87 cases were evaluated in the study. The final diagnoses of renal lesions included the following: RCC ($n = 35$, 32.7%), TCC ($n = 3$, 2.8%), lymphoma ($n = 8$, 7.5%), plasmacytoma ($n = 1$, 0.9%), Angiomyolipoma (AML) ($n = 13$, 12.1%), pyelonephritis ($n = 10$, 9.3%), pseudo-tumor in chronic kidney disease (CKD) ($n = 4$, 3.7%); Bosniak (Type I) cyst ($n = 22$, 20.5%), Bosniak (Type II & II F) cyst ($n = 9$, 8.4%), and Bosniak (Type III) cyst ($n = 2$, 1.8%).

A total of 49 lesions (45.8%) were confirmed by pathology. Thirty-seven patients underwent radical resection, 3 patients underwent nephron-sparing surgery, and 9 lesions were confirmed by biopsy. The rest of the lesions had been followed up. They were stable over a minimum period of 6 months on US or CT examinations. Lesions characteristics are summarized in Table 2.

3.2. Conventional MRI

There were 74 (69.2%) solid lesions and 33 (30.8%) cystic lesions. Two lesions of Bosniak type IV cysts were classified in the solid group. Out of 60 benign lesions 33 were cystic (58.92%) and 27 were solid (39.28%). All 47 malignant renal lesions were solid.

The signal intensity of the lesions on T1, T2WI and fat-suppression T1 images was recorded. On T1WI, 75 lesions (70.1%) elicited low signal, 3 lesions (2.8%) (hemorrhagic cysts) elicited high signal and 29 lesions (27.1%) (10 RCC, 13 AML, 6 hemorrhagic cysts) elicited mixed high and low signal.

13/32 high T1 signal intensity lesions showed signal drop at T1 fat-suppression sequence, and they were diagnosed as AML. 3/32 high T1WI lesions and 16/32 mixed high and low T1 signal intensities lesions showed no suppression in hemorrhagic cysts and masses.

21/35 (60%) RCC lesions, showed heterogeneous enhancement pattern. In such lesions, ROI was placed at the solid enhancing portion in order to measure the cellular part of the tumor.

3.3. Diffusion imaging and ADC value

The ADC values of normal renal parenchyma and renal lesions are listed in Table 3.

There was statistical significance difference between ADC value of normal renal parenchyma with that of benign and malignant renal lesions (*P* value < 0.0001).

ADC values differed significantly between solid (74/107, 69.2%) and cystic lesions (33/107, 30.8%) (*P* value < 0.0001). There was a significance difference between ADC values of all benign (60/107, 56%) and malignant renal lesions (47/107, 44%) (*P* value < 0.0001) but not between benign solid (27/74, 36.5%) and malignant solid renal lesions (47/47, 63.5%) (*P* value = 0.784) (Table 4).

The highest ADC value of all lesion was that of Bosniak I cysts ($n = 22$). Their ADC value ranged from 2.66 to 3.90×10^{-3} mm^2/s (mean 3.1 ± 0.53). There were 9 hemorrhagic cysts (Bosniak II, IIF), and their ADC value ranges from 0.63 to 2.31×10^{-3} mm^2/s (mean 1.51 ± 0.56). We have 2 (Bosniak III) cysts, and their ADC values are 2.01 and 2.22×10^{-3} mm^2/s. There was a significant difference between the ADC values of Bosniak I simple cysts and ADC of Bosniak II and II F hemorrhagic cysts (*P* value < 0.001).

The ADC value of RCC lesions ($n = 35$) ranged from 1.01 to 1.88×10^{-3} mm^2/s (mean 1.42 ± 21) (Figs. 1 and 2). The mean ADC values of TCC ($n = 3$) and lymphoma lesions ($n = 8$) were statistically lower than those of RCC.

3/6 patients diagnosed with AMLs have tuberous sclerosis. ALL 13 AML lesions are fat containing, and their ADC values ranged from 0.47 to 1.6×10^{-3} mm^2/s (mean 0.95 ± 0.29).

Table 2 Lesions characteristics of the study group ($n = 107$).

Diagnosis	No of patients	No and % of lesions	Mean size in cm	Confirmed by pathology
Cystic lesions	31	33(30.8%)		
–Bosniak I	20	22(20.5%)	3.2 ± 0.8	–
–Bosniak II, IIF	9	9(8.4%)	4.6 ± 2.1	–
–Bosniak III	2	2(1.8%)	11.5 ± 10.6	2
Solid lesions	56	74(69.2%)		
–RCC	35	35(32.7%)	6.32 ± 3.4	35
–TCC	3	3(2.8%)	3.9 ± 1.73	3
–Lymphoma	4	8(7.5%)	2.6 ± 0.8	8
–Plasmacytoma	1	1(0.9%)	18	1
–Angiomyolipoma	6	13(12.1%)	3.2 ± 2.5	–
–Pyelonephritis	5	10(9.3%)	4.06 ± 1.7	–
–Pseudotumor in CKD	2	4(3.7%)	4 ± 0.3	–
Total	87	107		49

Table 3 Apparent diffusion coefficient (ADC) values of different groups in the study.

Study group	No	Minimum ADC value	Maximum ADC value	Mean ADC value
Normal renal parenchyma	85	1.6	2.7	2 ± 0.16
Cystic lesions	33			
–Bosniak I	22	1.92	4.08	3.11 ± 0.54
–Bosniak II, IIF	9	0.63	2.31	1.51 ± 0.56
–Bosniak III	2	2.01	2.22	2.11 ± 0.14
Solid lesions	74			
–RCC	35	1.01	1.88	1.42 ± 0.22
–TCC	3	1.11	1.18	1.15 ± 0.3
Plasmacytoma	1		1.12	
–Lymphoma	8	0.58	1.21	0.75 ± 0.2
–AML	13	0.47	1.6	0.95 ± 0.3
–Pyelonephritis	10	0.8	1.42	1.11 ± 0.3
–Pseudotumor in CKD	4	2.5	2.66	2.59 ± 0.6

Table 4 Comparison between mean ADC values of different groups of the study.

Normal renal parenchyma 2 ± 0.16	Benign 2.09 ± 1.03	*P* value <0.0001*
Normal renal parenchyma 2 ± 0.16	Malignant 1.3 ± 0.32	<0.0001*
All benign 2.00 ± 1.03	Malignant 1.28 ± 0.32	<0.0001*
Benign solid 1.25 ± 0.628	Malignant 1.28 ± 0.32	0.79
Cystic 2.62 ± 0.89	Solid 1.27 ± 0.45	<0.0001*
Bosniak I cyst 3.11 ± 0.54	Bosniak II & IIF cyst 1.51 ± 0.56	<0.0001*
RCC 1.42 ± 0.22	TCC 1.15 ± 0.3	<0.05
RCC 1.42 ± 0.22	Lymphoma 0.75 ± 0.2	<0.0001*
RCC 1.42 ± 0.22	AML 0.95 ± 0.3	0.0004*
RCC 1.42 ± 0.22	PN 1.11 ± 0.3	0.0004*
RCC 1.42 ± 0.22	Pseudo-tumor CKD 2.59 ± 0.6	<0.0001*

Data are expressed as mean ± SD. **$p < 0.01$ = highly significant.

Ten lesions were diagnosed as pyelonephritis, and their ADC value ranged from 0.8 to 1.42 × 10^{-3} mm^2/s (mean 1.1 ± 0.26) (Fig. 3).

The mean ADC value for pseudo-tumors in CKD ($n = 4$) was 2.6 ± 0.06 × 10^{-3} mm^2/s. It was significantly higher than that of RCC ($P < 0.0001$) as well as normal renal parenchyma (Fig. 4).

3.4. ADC cutoff value for differentiating benign from malignant lesions

ROC analysis revealed AUC = 0.758%, 95% CI: 0.668–0.849, $p = 000$ at an ADC cutoff value of ⩽1.88 × 10 mm^2/s, sensitivity and specificity for diagnosis of malignant were 100% and 48.3% respectively (Fig. 5).

4. Discussion

DW-MRI has a rising role in the characterization of renal masses (7). In biologic tissues that are highly cellular (such as tumors), the higher density of cell membranes restricts the diffusion of water protons. This restriction to diffusion manifests as high signal intensity on DWI and corresponding lower ADC (8).

In this study, we investigated the diagnostic potential of DWI and quantitative assessment of ADC value for the characterization of renal lesions and differentiation into benign and malignant.

There is no consensus regarding the optimal *b*-values to be used in renal imaging (9). An image of low *b*-value (0–300 s/mm^2) has higher SNR, less distortion, but less diffusion weighting. Conversely, high *b*-factor (800 s/mm^2) images have more diffusion weighting but suffer from low signal-to-noise ratio and image distortion. Some researchers have recommended using *b* value >400 s/mm^2 because it can reduce "T2 shine-through" and intra-voxel perfusion effects (10). This study was conducted with *b* values (0, 600 and 800). Similar *b* values were used in the previous reports (10–13).

The main drawback of DWI is the lack of standardization, and the variability of ADC values is attributed mainly to different sample sizes, *b* values, coil systems, breath-hold versus free breathing, and field strengths used for MRI (14).

In normal renal parenchyma we recorded a mean ADC value of 2.00 ± 0.16 × 10^{-3} mm^2/sec). In previous reports, the mean ADC value of normal renal parenchyma ranged from 1.72 to 2.65 × 10^{-3} mm^2/s (1,15–17).

We found a significant difference in the mean ADC between malignant and benign renal lesions (*P* value < 0.0001). This was in concordance with previous studies (18–20).

The cutoff ADC value obtained and used for differentiation between benign and malignant lesions was 1.88 × 10^{-3} mm^2/s. It revealed a sensitivity of 100% and specificity of 48.3%. Despite the statistically significant difference in the mean

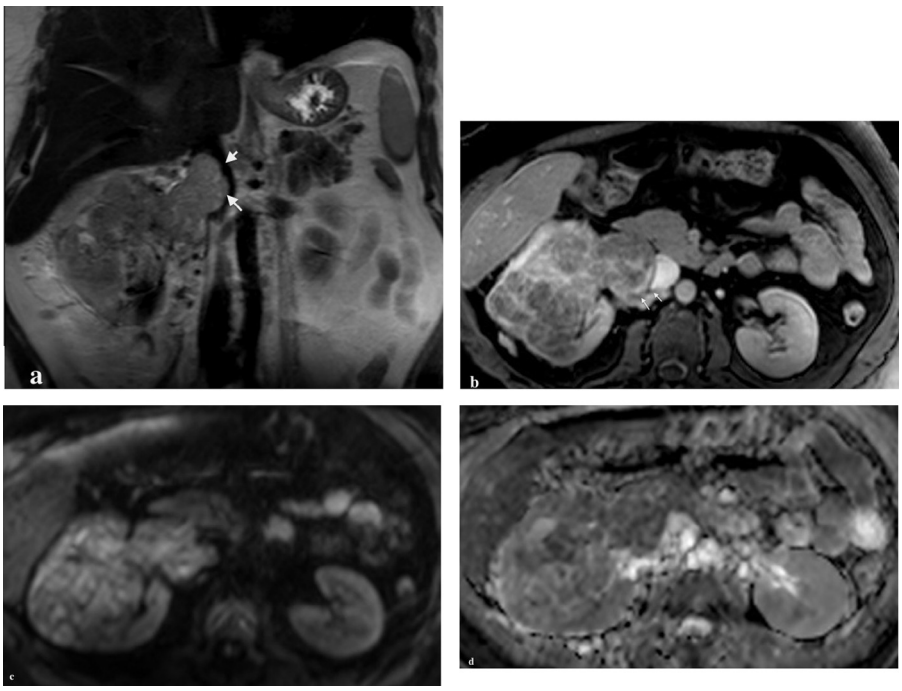

Fig. 1 A 52-year-old female with clear cell RCC. (a) Coronal T2WIs and (b) Postcontrast axial T1WIs show large right renal mass invading the RV and IVC (arrows), (c) DWI at *b* value of 800 and (d) ADC map show restricted diffusion of the lesion, and the ADC is 1.5×10^{-3} mm^2/sec.

ADC values of benign and malignant lesions, there was an overall considerable overlap between the two groups rendering ADC measurement of lower value in distinguishing benign from malignant renal lesions. Based on ADC measurement alone, 29/60 (48.3%) benign cases were falsely diagnosed as malignant.

RCC can have a varied appearance on DWI owing to differing degrees of cellularity and elements of necrosis, cystic change, or hemorrhage. In such complex renal masses, solid enhancing tumor components demonstrate lower ADC values than necrotic or cystic regions (12). In the current work, 60% of RCCs showed heterogeneous restriction of diffusion, with solid enhancing regions demonstrated moderate restriction and T2 hyperintense cystic components demonstrated free diffusion.

Likewise, TCC displays restricted diffusion due to high cellularity; they stand out as areas of bright signal against a background of suppressed signal within the collecting system and adjacent normal renal parenchyma on high *b*-value images while demonstrating low signal on the corresponding ADC map (20).

The present study demonstrated that the ADC value of TCC was significantly lower than for normal renal parenchyma and RCC (P value < 0.0001, 0.05 respectively). This was in agreement with Yoshida et al., who reported lower ADC values in TCC ($1.29 \pm 0.15 \times 10^{-3}$ mm^2/s), when compared with renal parenchyma ($2 \pm 0.16 \times 10^{-3}$ mm^2/s) (21). Similarly, in a study by Paudyal et al., they have found that ADC value was significantly higher for RCC than for TCC (22). Contrasting results have been reported by Sevcencoa et al., the authors have found no difference in ADC value between RCC and TCC (23). Similar to our study, because of the limited number of included TCC, conclusions cannot be drawn regarding the value of DW-MRI for distinguishing between RCC and TCC.

Renal lymphoma tends to show diffusion restriction (24). In these series, 8 lesions were easily seen with high signal on DWI. They had the lowest ADC values among all malignant lesions with a mean value of $0.74 \pm 0.2 \times 10^{-3}$ mm^2/s, which is in a range of the previously reported values for lymphoma (0.64 to 0.76×10^{-3} mm^2/s) (25–27). The usefulness of ADC value measurement in the diagnosis of renal lymphoma and differential diagnosis from other hypo-enhancing renal masses such as papillary or chromophobe RCC, or metastasis has been suggested by Nguyen and Rakita. Moreover, they have found that DWI allowed better depiction of multiple lesions against a suppressed background signal (25).

AML is a common benign renal neoplasm that occurs in 0.3–3% of the population (1). AML is composed of variable amounts of fat, muscle tissue, and abnormal blood vessels. These tissues prevent the molecules of water from spreading freely, and causing a low ADC value (1). The ability to differentiate AMLs is especially urgent in patients with tuberous sclerosis, since AMLs develop in about 80% of these patients, and at the same time these patients are at increased risk of developing RCC (28).

The ADC value of AML is related to its fat content with gradually decreasing the ADCs of AML with inverse correlation of its fatty content (13,29). Only 13 lesions were diagnosed as AML in our study, all of them were fat containing AML. Hence, they were easily recognized on conventional MRI with typical fat components. Their mean ADC value ($0.95 \pm 0.3 \times 10^{-3}$ mm^2/s) was significantly lower than that of RCC, and our findings were in concordance with previous studies (11,12,18,19). Contrasting results have been reported by Kilickesmez et al., (29) who have found that mean ADC

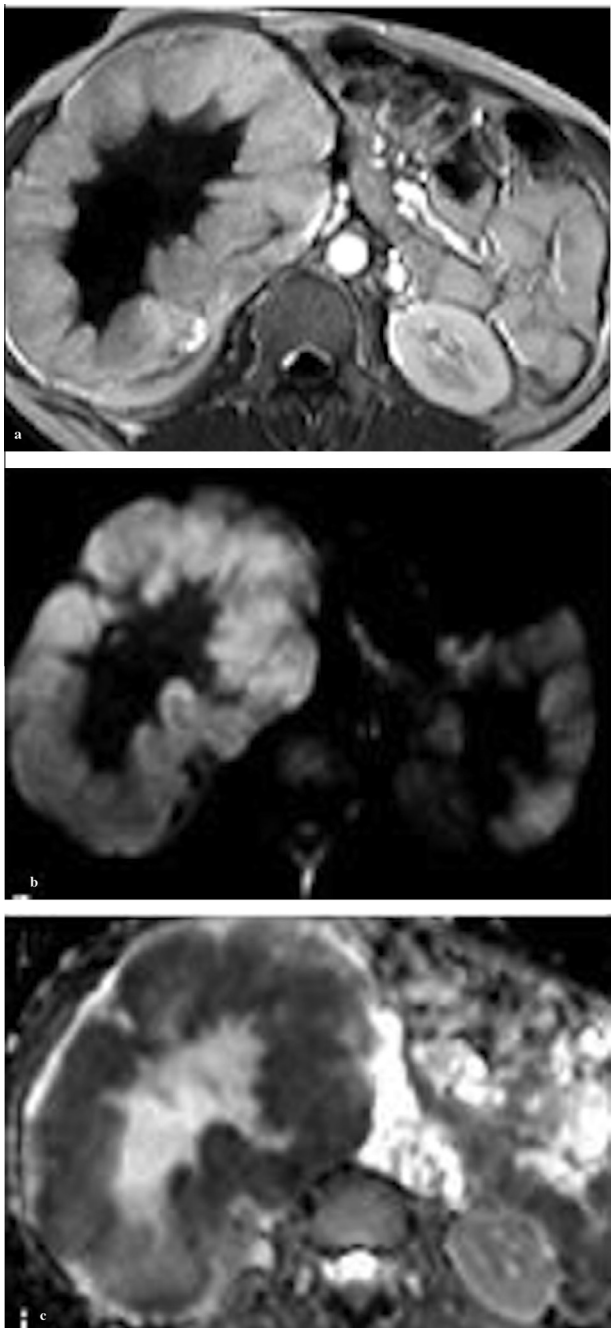

Fig. 2 A 37-year-old male with chromophobe RCC. (a) Post-contrast axial T1WIs show heterogenous enhancing large exophytic right renal lesion with nonenhancing central region. (b) DWI at *b* value of 800 and (c) ADC map show restricted diffusion of the peripheral solid part and facilitated diffusion of the central region. The ADC values of the peripheral solid component and central region are 1.27×0^{-3} mm^2/sec and 2.8×10^{-3} mm^2/sec respectively.

value was higher for AMLs (1.40 ± 0.21) than for RCCs (1.06 ± 0.39). Also Inci et al., (1) reported a mean ADC value of 1.19 ± 0.36 for 16 cases of AML, with no significant difference from RCCs (1.12 ± 0.23).

Renal infection and some associated complications also demonstrate restricted diffusion and should not be mistaken for malignancy. Pyelonephritis results in patchy non mass like areas of restricted diffusion in portions of the renal parenchyma, a finding that may relate to inflammatory cell infiltration and possible ischemic effects of infection (30). In this work, 10 lesions were diagnosed as multifocal pyelonephritis. The mean ADC value of all lesions was 1.11×10^{-3} mm^2/s ± 0.3, that was lower than mean ADC of normal renal parenchyma and RCC with statistical difference. This was in agreement with the findings of Goyal et al., who have found that the ADC values of inflammatory lesions were significantly lower than those of RCC, suggesting that DW-MRI may be an additional tool to distinguish between inflammatory and malignant renal lesions (31).

Owing to non-uniform patchy involvement in CKD (32–34), there may be nodular compensatory hypertrophy of the relatively spared renal parenchyma, leading to the formation of pseudo-tumors, which may produce mass effect in the form of contour abnormality or splaying/compressing the pelvicalyceal system (35). In our series, the mean ADC value of four lesions diagnosed as pseudo-tumor was 2.59 ± 0.62×10^{-3} mm^2/s, which was higher than the ADC values of RCCs (P value < 0.0001). This was in concordance with the previously reported value of $2.50 \pm 0.22 \times 10^{-3}$ mm^2/s (35). As perviously reported by Goyal et al. (35), we have found, that the surrounding renal parenchyma showed peripheral-based, wedge-shaped foci of restricted diffusion.

In our study, the highest ADC value of all lesions was that of simple renal cyst (Bosniak I). This could be attributed to their fluid content, with non-restricted motion of water molecules (29). Our findings were in concordance with previous reports (1,11,12,19).

Renal hemorrhagic cysts can sometimes display very low signal on the ADC map, a finding that may relate to the "T2 blackout" effects of an intrinsically T2 hypointense lesion and/or restricted diffusion in blood products (36). In this study, we compared the ADC values of simple renal cyst (Bosniak I) and hemorrhagic T1 hyperintense (Bosniak II, IIF) cysts, to rule out the effect of hemorrhagic content in ADC values variations. Similar to Sandrasegaran et al. (19), we have found that the mean ADC value of hemorrhagic cysts was lower than that of simple cysts, with statistical significant difference (P value < 0.0001).

In this study, the use of DWI and ADC measurement was particularly useful in diagnosis of renal lesions of 6 patients with renal insufficiency in whom contrast medium was not administrated for the fear of nephrogenic systemic fibrosis. DWI allowed for better depiction of pyelonephritis and TCC lesions. Furthermore, it confirmed the diagnosis of pseudo-tumor in CKD and excluded the possibility of RCC, owing to lack of diffusion restriction and high ADC value.

Limitations of this study include relatively poor spatial resolution and anatomic localization with the use of high *b* value DWI, together with small number of patients sample in some groups such as TCC and plasmacytoma which to some extent limit the power of statistical analysis.

In conclusion, DWI and quantitative ADC measurements could be easily added to a routine MR imaging protocol. It had the advantages of being fast and not requiring a contrast administration. However, there is an overlap between the ADC values of benign and malignant lesions. Thus ADC measurement could not predict with certainty if the lesions were benign or malignant. DW-MRI should be interpreted in

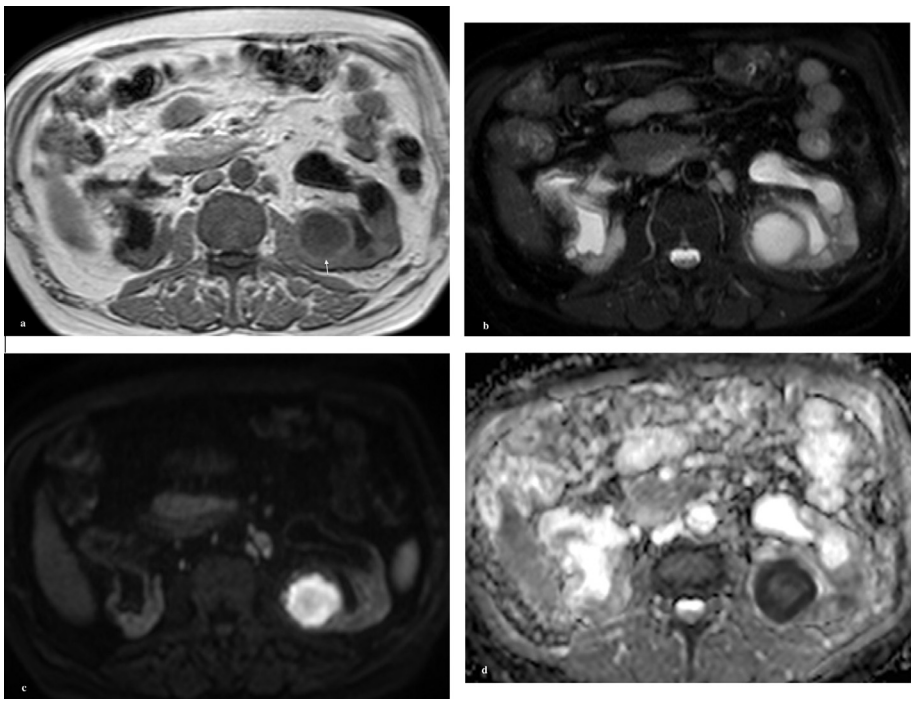

Fig. 3 A 50-year old diabetic male patient with left renal pyelonephritis. Gd-DTPA was not administrated due to impaired kidney function. (a) Axial fat-suppression T2WI demonstrates enlarged left kidney, showing a well defined cystic lesion with two tiny foci of subtle hyperintense T2 signal. (b) DWIs at *b* value 800 and (c) ADC map show marked restricted diffusion of the lesion, with ADC value of 0.6×10^{-3} mm^2/sec. Very bright signal on diffusion and dark signal on ADC map are characteristic of renal abscess. The two foci show diffusion restriction as well, and they are better depicted on ADC images (arrowed).

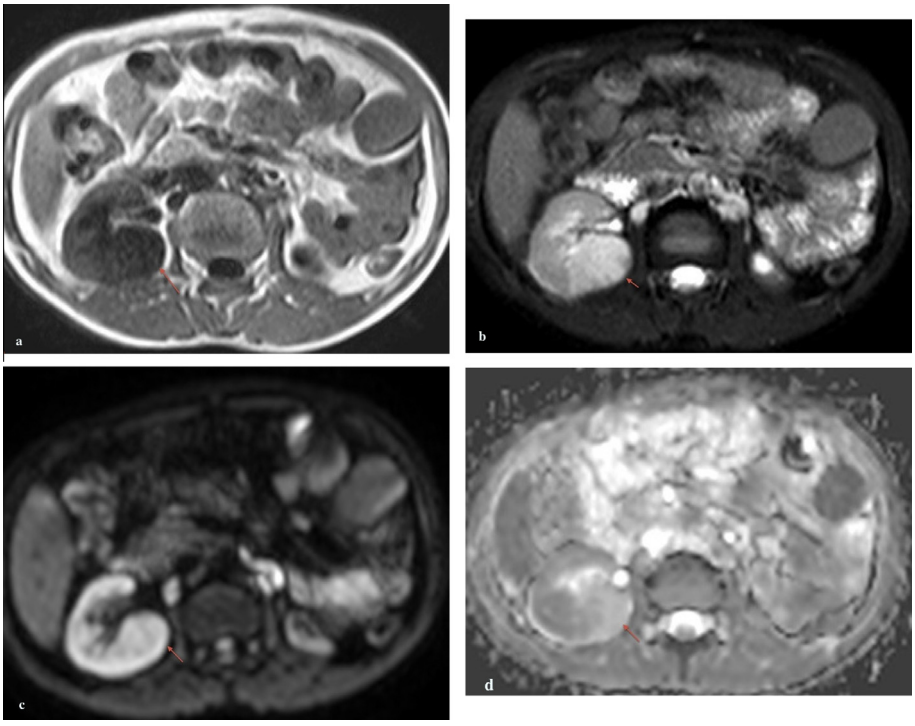

Fig. 4 A 17-year old female patient with pseudo-tumour in CKD. Gd-DTPA was not administrated owing to impaired kidney function as a result of Systemic Lupus Erythematosus (SLE). (a) Axial T1WI shows a nodular lesion at the medial aspect of the right kidney mildly hypointense to surrounding parenchyma. The lesion is hyperintense on axial fat suppression T2WI (b). Note small atrophic left kidney. (c and d) DWI at *b* value of 800 and ADC map demonstrate absence of diffusion restriction (ADC value is 2.61×10^{-3} mm^2/sec). There are wedge areas of diffusion restriction in the surrounding renal parenchyma.

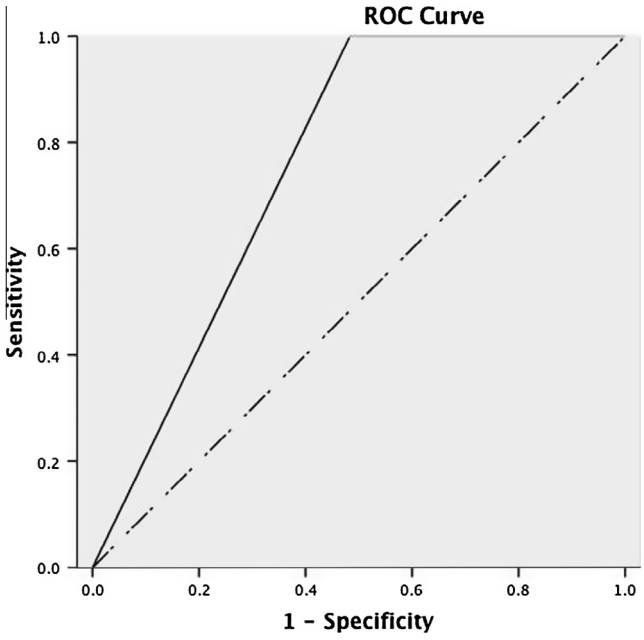

Fig. 5 Receiver operating characteristic (ROC) curve of the cutoff ADC value used for differentiating malignant from benign renal tumors which is 1.88×10^{-3} mm^2/sec with an area under the curve (AUC) = 0.758%.

conjunction with conventional MRI sequences to allow for better assessment of renal lesions.

Conflict of interest

The authors declared no conflict of interest.

References

(1) Inci E, Elif H, Sibel A, Tan C. Diffusion-weighted magnetic resonance imaging in evaluation of primary solid and cystic renal masses using the Bosniak classification. Eur J Radiol 2012;81:815–20.
(2) Willatt JM, Hussain HK, Chong S, Kappil M, Azar SF, Liu PS, et al. MR imaging in the characterization of small renal masses. Abdom Imaging 2014;39:761–9.
(3) Giannarini G, Petralia G, Thoeny HC. Potential and limitations of diffusion-weighted magnetic resonance imaging in kidney, prostate, and bladder cancer including pelvic lymph node staging: a critical analysis of the literature. Eur Urol 2012;61:326–40.
(4) Baliyan V, Das CJ, Sharma S, Gupta A. Diffusion-weighted imaging in urinary tract lesions. Clin. Radiol. 2014;69:773–82.
(5) Bosniak MA. The current radiological approach to renal cysts. Radiology 1986;158:1–10.
(6) Israel GM, Hindman N, Bosniak MA. Evaluation of cystic renal masses: comparison of CT and MR imaging by using the Bosniak classification system. Radiology 2004;231:365–71.
(7) Koh D-M, Collins D. Diffusion-weighted MRI in the body: applications and challenges in oncology. Am. J. Roentgenol. 2007;188:1622–35.
(8) Gilet AG, Kang SK, Danny Kim, Chandarana H. Advanced renal mass imaging: diffusion and perfusion MRI. Curr Urol Rep 2012;13(1):93–8.
(9) Taouli B, Koh DM. Diffusion-weighted MR imaging of the liver. Radiology 2010;254(1):47–66.
(10) Yoshikawa T, Kawamitsu H, Mitchell DG. ADC measurement of abdominal organs and lesions using parallel imaging technique. AJR Am J Roentgenol 2006;187:1521–30.
(11) Taouli B, Thakur R, Mannelli L, Babb J, Kim S, Hecht E. Renal lesions: characterization with diffusion-weighted imaging versus contrast-enhanced MR imaging. Radiology 2009;251:398–407.
(12) Zhang J, Tehrani YM, Wang L, Ishill NM, Schwartz LH, Hricak H. Renal masses: characterization with diffusion-weighted MR imaging—a preliminary experience. Radiology 2008;247:458–64.
(13) Razek AA, Farouk A, Mousa A, Nabil N. Role of diffusion-weighted magnetic resonance imaging in characterization of renal tumors. J Comput Assist Tomogr 2011;35(3):332–6.
(14) Zhang JL, Sigmund EE, Chandarana H, et al. Variability of renal apparent diffusion coefficients: limitations of the monoexponential model for diffusion quantification. Radiology 2010;254:783–92.
(15) Cova M, Squillaci E, Stacul F, et al. Diffusion-weighted MRI in the evaluation of renal lesions: preliminary results. Br J Radiol 2004;77:851–7.
(16) Carbone SF, Gaggioli E, Ricci V, Mazzei F, Mazzei MA, Volterrani L. Diffusion-weighted magnetic resonance imaging in the evaluation of renal function: a preliminary study. Radiol Med 2007;112:1201–10.
(17) Agnello F, Roya C, Bazille, Midiri G, Charles T, Lang H. Small solid renal masses: characterization by diffusion weighted MRI at 3 T. Clin Radiol 2013;68:301–8.
(18) Doganay S, Kocakoc E, Aglamis S, Akpolat N, Orhan I. Ability and utility of diffusion-weighted MRI with different b values in the evaluation of benign and malignant renal lesions. Clin Radiol 2011;66:420–5.
(19) Sandrasegaran K, Sundaram CP, Ramaswamy R, Akisik FM, Rydberg MP, Lin C, et al. Usefulness of diffusion-weighted imaging in the evaluation of renal masses. AJR Am J Roentgenol 2010;194:438–45.
(20) Cogley JR, Dustin DN, Peter MG, Dmitry R. Diffusion-weighted MRI of renal cell carcinoma, upper tract urothelial carcinoma, and renal infection: a pictorial review. Jpn J Radiol 2013;31:643–52.
(21) Yoshida S, Masuda H, Ishii C, Tanaka H, Fujii Y, Kawakami S, et al. Usefulness of diffusion-weighted MRI in diagnosis of upper urinary tract cancer. AJR Am J Roentgenol 2011;196:110–6.
(22) Paudyal B, Paudyal P, Tsushima Y, et al. The role of the ADC value in the characterization of renal carcinoma by diffusion-weighted MRI. Br J Radiol 2010;83(988):336–43.
(23) Sevcencoa S, Heinz-Peerb G, Ponholdb L, Javorb D, Kuehhasa FE, Klinglera HC, et al. Utility and limitations of 3-Tesla diffusion-weighted magnetic resonance imaging for differentiation of renal tumors. Eur J Radiol 2014;83:909–13.
(24) Ganeshan D, Iyer R, Devine C, Bhosale P, Paulson E. Imaging of primary and secondary renal lymphoma. AJR 2013;201:W712–9.
(25) Ngueyen DD, Rakita D. Renal lymphoma: MR appearance with diffusion-weighted imaging. J Comput Assist Tomogr 2013;37(5):840–2.
(26) Zhang Y, Chen J, Shen J, Zhong J, Ye R, Liang B. Apparent diffusion coefficient values of necrotic and solid portion of lymph nodes: differential diagnostic value in cervical lymphadenopathy. Clin Radiol 2013;68:224–31.
(27) Wu X, Petroveaara H, Dastidar P, Vornanen M, Paavolainen L, Marjomaki V, et al. ADC measurements in diffuse large B-cell lymphoma and follicular lymphoma: a DWI and cellularity study. Eur J Radiol 2013;82:158–64.
(28) Nikken JJ, Krestin Gp. MRI of the kidney: state of the art. Eur Radiol 2007;17:2780–93.
(29) Kilickesmez O, Inci E, Atilla S, Tasdelen N, Yetimo B, Yencilek F, et al. Diffusion-weighted imaging of the renal and adrenal lesions. J Comput Assist Tomogr 2009;33(6):828–33.

(30) Bittencourt LK, Matos C, Coutinho AC. Diffusion-weighted magnetic resonance imaging in the upper abdomen: technical issues and clinical applications. Magn Reson Imaging Clin N Am 2011;19:111–31.
(31) Goyal A, Raju Sh, Ashu SB, Shivanand G, Amlesh S. Diffusion-weighted MRI in inflammatory renal lesions: all that glitters is not RCC! Eur Radiol 2013;23(1):272–9.
(32) Remuzzi G, Ruggenenti P, Benigni A. Understanding the nature of renal disease progression. Kidney Int 1997;51:2–15.
(33) Alpers CE. The kidney. In: Kumar V, Abbas AK, Fausto N, Aster JC, editors. Rob-bins and Cotran pathologic basis of disease. Philadelphia, PA: Saunders Elsevier; 2010. p. 905–69.
(34) Nadasdy T, Sedmak D. Acute and chronic tubulointerstitial nephritis. In: Jennette JC, Olson JL, Schwartz MM, Silva FG, editors. Heptinstall's pathology of the kidney. Philadelphia, PA: Lippincott Williams & Wilkins; 2007. p. 1084–137.
(35) Goyal A, Sharma R, Bhalla AS, Gamanagatti S, Seth A. Pseudotumours in chronic kidney disease: can diffusion-weighted MRI rule out malignancy. Eur J Radiol 2013;82:1870–6.
(36) Kim S, Jain M, Harris AB, Lee VS, Babb JS, Sigmund EE, et al. T1 hyperintense renal lesions: characterization with diffusion weighted MR imaging versus contrast-enhanced MR imaging. Radiology 2009;251:796–807.